PRINT ISSN 1119-8362
Electronic ISSN 1119-8362

Full-text Available Online at
https://www.ajol.info/index.php/jasem
http://ww.bioline.org.br/ja

J. Appl. Sci. Environ. Manage.
Vol. 25 (8) 1441-1448 August 2021

Acetylcholine and Rivastigmine as Corrosion Inhibitors of Cu – Sn - Zn – Pb Alloy in Hydrochloric Acid Environment: DFT & Electrochemical Approach

[1]*UGI, BU; [1]BASSEY, VM; [2]OBETEN, ME; [3]ADALIKWU, SA; [1]OMALIKO, EC; [1]OBI, DN

*[*1]Department of Pure & Applied Chemistry, University of Calabar, P. M. B. 1115, Calabar, Nigeria.*
[2]Department of Chemistry, Cross River State University of Technology, Calabar, Nigeria
[3]Department of Chemistry, College of Education Akamkpa, Nigeria
**Corresponding Author Email: ugibenedict@gmail.com; Tel: +234706 792 1098*

ABSTRACT: The study on the action of Acetylcholine and Rivastigmine as Corrosion Inhibitors of Cu – Sn - Zn – Pb Alloy in Hydrochloric Acid Environment was carried out using density functional theory, electrochemical impedance spectroscopy, Potentiodynamic polarization, Scanning electron microscopy and weight loss. The result revealed that both Acetylcholine and Rivastigmine expired drugs were good inhibitors of Cu – Sn - Zn – Pb Alloy in Hydrochloric Acid Environment. This was confirmed from results of weight loss (99.1 % and 95.0 %), electrochemical impedance spectroscopy (EIS) (92.5 % and 91.8 %), and Potentiodynamic polarization (97.4 % and 87.1 %). Both inhibitors were able to increase the charge transfer resistance and corrosion current densities of the electrical solution and reduce the double layer capacitance of the metal – solution interface. Inhibition was as a result of adsorption of inhibitor molecules on the Cu – Sn - Zn – Pb surface. Thermodynamically, inhibitors showed greater stability on metal surface, spontaneous in the forward direction and reduction in level of disorderliness. Inhibitors demonstrated a mixed type inhibition while physical adsorption mechanism was proposed for the inhibitor – metal interaction. Langmuir adsorption isotherm was obeyed as data fitted adequately to the isotherm and regression coefficient was approximately unity. A monolayer adsorption was deduces.

DOI: https://dx.doi.org/10.4314/jasem.v25i8.24

Dates: Received: 10 May 2021; Revised: 28 June 2021; Accepted: 01 July 2021

Keywords: Corrosion, isotherm, Rivastigmine, Alloy, Adsorption, Thermodynamics

In order to transform a refined material (in this case a metal) into a chimerically stabled form which could be oxide, hydroxide, or sulfide, corrosion is always involved (Ammen 2000). Corrosion is seen as the gradual destruction of materials by chemical and/or electrochemical reaction in an environment (Ammen 2000; Brady *et al.*, 2002). The most frequently occurring type of corrosion is electrochemical corrosion in which the oxidation process $M \rightarrow M^{+} + e^{-}$ is facilitated by the presence of a suitable electron acceptor, sometimes referred to as a depolarizer. Corrosion can easily be influenced by factors like metals type, relative size of anode and environment (temperature, humidity, salinity, etc.) (Ammen 2000; Dagdag *et al.*, 2019). Green corrosion inhibitors are one of the five ways to protect materials against corrosion especially since they adsorb on the surface of the material to form protective film which displace water and protect it against damage (Ammen 2000; Brady *et al.*, 2002; Dagdag *et al.*, 2019). Substances containing heteroatoms (O, N, and S, etc.) which are the possible active centers for the process of adsorption are identified with higher basicity and electron density hence, could demonstrate features of a good inhibitor (Dagdag *et al.*, 2019; Davanya *et al.*, 2020; Davis 2000). The performance of a green inhibitor is related to the chemical structure and physicochemical properties of the compound like functional groups, electron density at the donor atom, p-orbital character, and the electronic structure of the molecule (Dagdag *et al.*, 2019). The aim of this research is to understand the possible inhibition strength of Acetylcholine and Rivastigmine expired drugs on Cu – Sn - Zn – Pb Alloy (Gun Metal) in Hydrochloric Acid Environment, their mechanism of adsorption and thermodynamic effects on the inhibitors.

MATERIAL AND METHODS

Description of inhibitor used: A typical green inhibitor is that employed in this research (Figs. 1a – b), and their usage for this research boils down to the reasons stated earlier and not undermining also the fact that there is limited work on these two in the area of corrosion science and their possible potency in corrosion inhibition as green inhibitors.

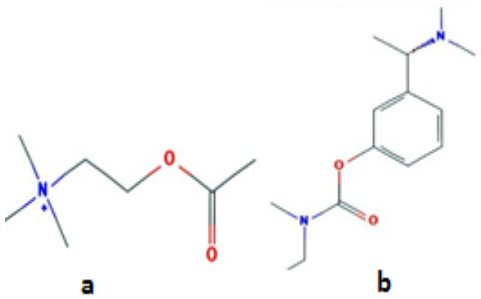

Fig. 1. (a) Acetylcholine (b) Rivastigmine

**Corresponding Author Email: ugibenedict@gmail.com; Tel: +234706 792 1098*

Gunmetal has been used earlier in the making of guns, including mirror cases, church doors, fonts and statues. Of late, it is used in the manufacture of intricate castings, valves, gears and bearings where loads and speeds are moderate[5]. Its elemental composition is described as, Cu = 88 %, Zn = 3 %, Sn =7 %, Pb =2 %. (European Copper Inst.; Faiza *et al.*, 2020).

Metal treatment and inhibitor preparation: The Gunmetal (Cu – Sn - Zn – Pb Alloy) was obtained from System Metals Industries Limited, Nigeria. The metal was resized to a dimension of 5.0 x 1.5 x 5.0 cm for weight loss analysis and 1 x 1 cm for electrochemical analysis. A 5005TV model electric polish machine was used for the mirror surface polishing of the metal through the help of different grades of Silicon Cabide papers from rough to smooth (800, 1000, 1200 and 1500 grits). Polished metals were preserved in a desiccator for use to avoid further corrosion. The expired drugs, Acetylcholine and Rivastigmine obtained from BEZ pharmacy were ground to obtain a small surface area that will allow for high absorption of solvent. 10 g each of the grounded sample was weighed separately using a M1514GT model digital electronic weighing balance and digested in a 1000 ml volumetric flask containing 1.5 M hydrochloric acid solution. After 24 hours, the solution was used to prepare different concentrations of the inhibitor in ppm (300, 500, 500, 700, 900 and 1200 ppm) for the corrosion test.

Weight loss procedure and experimentation: Different concentrations of inhibitor stock solution (300, 500, 500, 700, 900 and 1200 ppm) prepared to 100 ml of 1.5 M solution of HCl through the aid of a 100 ml volumetric flask was emptied to an already marked 100 ml conical flask. The already prepared Cu – Sn - Zn – Pb alloy from the desiccator were washed in distilled water, degreased in ethanol, rinsed in acetone and air dried 8-10. Initial weight of metals were recorded though the aid of an electronic weighing balance and immediately immersed in the different inhibitor in the 100 ml flask. After every 24 hours, the metals were removed, washed in distilled water, degreased in ethanol, rinsed in acetone and air dried and the weight recorded. This process continued for 120 hours (5 days). The same procedure was maintained for the weight loss experimentation of Rivastigmine. Corrosion rate of metal was determined from the slope of the plot of weight loss of metal against time of immersion, while surface coverage and inhibition efficiency of inhibitor were determined following Equation 1 and 2.

$$\vartheta = 1 - [b^{-a}] \qquad (1)$$

$$\%\delta = \frac{1-[b^{-a}]}{\frac{1}{100}} \qquad (2)$$

Where ϑ is the surface coverage, "b" is the blank solution, "a" the inhibitor solution, δ the inhibition efficiency.

Electrochemical assembly and experimentation: In this experiment, the Cu – Sn - Zn – Pb alloy was used as the working electrode (WE), SCE was introduced as the reference electrode (RE) and the counter electrode (CE) was platinum foil. A small sinusoidal perturbation of fixed frequency was applied to the system and the impedance at each frequency was evaluated from the measured response. Gamry Reference 600 potentiostart/galvanostart inclusive of a Gamry framework EIS300 system. Echem analyst software was used to analyze the fitting of the data. . Electrochemical tests were conducted within a frequency of 10 Hz - 100,000 Hz within potentiodynamic conditions, with an amplitude of 5 mV, involving alternating current signal at E_{corr}. All experiments were conducted every 60 min with and without various concentrations of the inhibitors. From the R_{ct} obtained, the retardation efficiency was calculated using Equation 3 and 4.

$$\vartheta = 1 - [R_0{}^{-u}] \quad \ldots \qquad (3)$$

$$\%\delta = \frac{1-[R_0{}^{-u}]}{\frac{1}{100}} \qquad (4)$$

Where Ro and u represent the charge transfer resistance without and with the inhibitors, δ the inhibition efficiency and ϑ is the surface coverage.

Density functional theory (DFT): Quantum chemical calculations was adopted in the Density Functional Theory. Material Studio (version 9.0) was used for this theoretical work. The Vamp and Dmol[3] programs were used in the quantum calculations. For the Vamp, theoretical calculations were carried out at the Restricted Hartree-Fock level (RHF) using the Hamiltonian parametric method 3 (PM3), which is based on the neglect of diatomic differential overlap approximation. The Dmol[3] is a program which make use of the density functional theory (DFT) with a numerical radial function basis set to calculate the electronic properties of molecule's clusters.

Morphology examination: A scanning electron microscope (model JSM-5600 LV) was used to analyze the morphology of the Cu – Sn - Zn – Pb alloy surface without and with 300 ppm and 1500 ppm inhibitor solutions. A metal stub was used to carry the Cu – Sn - Zn – Pb alloy sample and in order to enhance conductivity, gold was sputtered on sample while the images taken at an accelerating voltage of 10 kV.

RESULT AND DISCUSSION

Weight loss analysis: Results from weight loss analysis always explain the possibility of the metal to withstand the aggressive nature of the acidic solution

with varying concentrations of inhibitor solutions. The greater the weight loss, the greater the inefficiency of the inhibitor solution used. From Table 1, it was observed that the corrosion rate was decreasing geometrically with increasing inhibitor concentration. This is as a result of the adsorption of the inhibitors at various concentrations (Dagdag *et al.*, 2019; Go *et al.*, 2020; Idouhli *et al.*, 2019). This could also imply that stronger inhibition efficiencies as recorded (99.1 % and 95.0 %) were due to the large surface coverage area by the inhibitor molecules hence developing a perfect substitution reaction between the inhibitor molecules and those of the water molecules (which is a primary agent of corrosion) (Idouhli *et al.*, 2019; Majda *et al.*, 2020; McCafferty 2010; Ngobiri *et al.*, 2019).

Table 1. Weight loss parameters for the inhibition of Cu – Sn - Zn – Pb Alloy surface in HCl environment

	Acetylcholine (ACC)			Rivastigmine (RVM)		
Conc.	CR (mg/cm2/h)	θ	% IE	CR (mg/cm2/h)	θ	% IE
Blank	0.936	-	-	0.936	-	-
300 ppm	0.402	0.571	57.1	0.298	0.682	68.2
500 ppm	0.365	0.610	61.0	0.277	0.704	70.4
700 ppm	0.211	0.775	77.5	0.142	0.848	84.8
900 ppm	0.153	0.837	83.7	0.025	0.973	97.3
1500 ppm	0.047	0.950	95.0	0.008	0.991	99.1

Electrochemical impedance spectroscopy: The extent of electrical resistant (impedance) by a metal in an inhibited solution is always determined from the EIS experimentation. The greater the resistance towards the applied current, the better the inhibitor strength and possibility to effectively reduce corrosion (Dagdag *et al.*, 2019; Gergely 2019; Obot *et al.*, 2019). Fig. 2 is the Nyquist plot that showed semicircles from the impedance. It was observed that the more the concentration of inhibitor is increased the further away the semicircles from the solution resistant point. Increased semicircles demonstrates increased in inhibition efficiency of the inhibitors and a possible electrical resistance of the solution (McCafferty 2010). This can be confirmed from the calculated values of the charged transfer resistance and double layer capacitance in Table 2 which are found to be increasing and decreasing, respectively with increased concentration. Results from the EIS were seen to be in accordance with those obtained from weight loss method, proving the effectiveness of both inhibitors in the corrosion control of Cu – Sn - Zn – Pb alloy in HCl environment. Data for the double-layer capacitance for the semicircles and inhibition efficiency were calculated using Eq. 6 as modified from Eq. 5.

$$C_{dl} = \frac{1}{\omega Z''} \quad \ldots \qquad (5)$$

where Z" is immaginay component of impedance at any frequency inside the semicircle and ω is the angular frequency. But $\omega = 2 * \pi * f_{max}$ (in Hz used for measurement of EIS).

Hence,

$$C_{dl} = \frac{1}{2\pi f_{max} Z''} \qquad (6)$$

Where f_{max} describe the maximun frequency of the semicircle and the π is 3.142

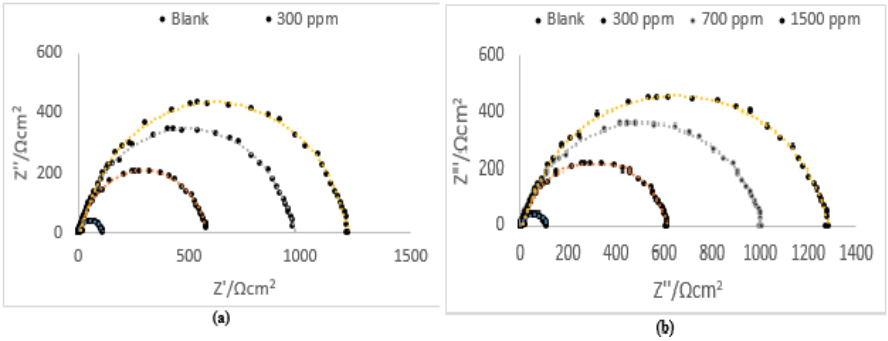

Fig. 2. Nyquist plots for the inhibition of Cu – Sn - Zn – Pb Alloy surface in HCl environment

Table 2. Electrochemical impedance parameters for the inhibition of Cu – Sn - Zn – Pb Alloy surface in HCl environment

	Conc.	R_{ct} (Ωcm^{-2})	C_{dl} (μFcm^{-2})	**Θ**	IE_R %
	Blank	99	1.61×10^{-5}	-	-
RVM	300 ppm	607	2.62×10^{-6}	0.837	83.69
	700 ppm	1005	1.58×10^{-6}	0.902	90.15
	1500 ppm	1311	1.21×10^{-6}	0.925	92.45
ACC	300 ppm	598	2.66×10^{-6}	0.835	83.45
	700 ppm	972	1.64×10^{-6}	0.898	89.82
	1500 ppm	1209	1.32×10^{-6}	0.918	91.81

Potentiodynamic polarization: One of the pieces of information often extracted from Potentiodynamic polarization scans is the corrosion current density, corrosion potential, cathodic and anodic slopes and calculated inhibition efficiency, amongst others. In line with these parameters, Table 3 was drawn out of the plots in Fig. 3. Results obtained revealed that the values of the corrosion current density decreased and this result is in accordance with those of weight loss. This explained a perfect adsorption of the inhibitor on the metal surface leading to shielding of corrosion active sites (Ngobiri *et al.*, 2019; Obot *et al.*, 2019; Ogunleye *et al.*, 2020). The corrosion potential was less than 80 mV, meaning that the potential shift towards negative, hence a mixed type inhibition is presented by the inhibitors. It also means that inhibitors should predominantly control the cathodic reaction (Majda *et al.*, 2020; Rodic and Milosey 2019; Sangeetha and Chinnakani 2020; Sehmi *et al.*, 2020). This is already revealed from the values of the cathodic and anodic slopes and the deflection of the plots in Fig. 3.

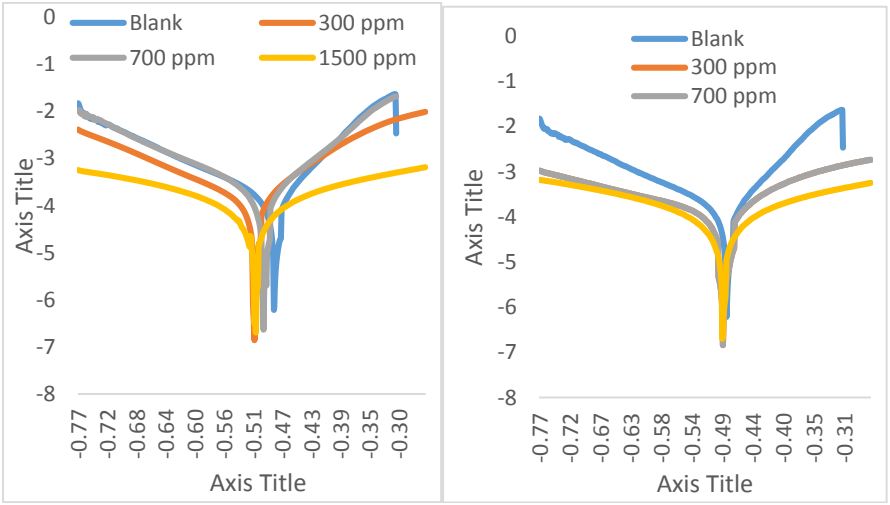

(a) (b)

Fig. 3. Tafel plots for the inhibition of Cu – Sn - Zn – Pb Alloy surface in HCl environment by rivastigmine (RVM) and acetylcholine (ACC)

Table 3. Potentiodynamic polarization parameters for the inhibition of Cu – Sn - Zn – Pb Alloy surface in HCl environment

	Conc.	I_{corr} ($mAcm^{-2}$)	E_{corr} (mV)	βc (mV/dec)	βa (mV/dec)	IEi (%)
	Blank	4.092	-368.7	311	297	-
RVM	300 ppm	0.721	-340.1	165	143	82.38
	700 ppm	0.552	-344.6	129	117	86.51
	1500 ppm	0.108	-328.8	100	69	97.36
ACC	300 ppm	1.421	-300.2	214	234	65.27
	700 ppm	0.979	-280.6	184	138	76.08
	1500 ppm	0.527	-241.0	166	91	87.12

Quantum Chemical Calculations (DFT): The optimized inhibitor structures showing the possible hetero atoms that could influence the inhibition process are shown in Fig. 4. Eqs 7 – 9 were adopted for the determination of the parameters (Shahzad *et al.*, 2020; Singh *et al.*, 2019).

$$\text{Energy gap } (\Delta E) = E_{HOMO} - E_{LUMO} \cdots \quad \ldots(7)$$

$$\text{Global hardness } (\eta) = \frac{(E_{HOMO} - E_{LUMO})}{2} \cdots \quad \ldots(8)$$

$$\text{Global softness } (S) = \frac{1}{2\left[\frac{(E_{HOMO} - E_{LUMO})}{2}\right]} \cdots \quad \ldots(9)$$

The result in Table 4 revealed that the inhibitors were strongly attached to the metal surface as binding energy was observed to be more positive (Dagdag *et al.*, 2019; Go *et al.*, 2020; Ogunleye *et al.*, 2020). However, the inhibition was better for the rivastigmine compared to acetylcholine, which is consequence upon its stronger adsorption on the surface of the metal. This is evident in their energy gap and the global softness parameters. The energy of the highest occupied molecular orbital was greater than that of the Lower unoccupied molecular orbital. This explained the easy transfer of inhibitor molecules to the metal and greater acceptance of charges from the surface, hence creating a balance in charges and inhibitor stability (Shahzad *et al.*, 2020; Sinh *et al.*, 2019; Solomon *et al.*, 2020). The high electrostatic potential as noticed with the rivastigmine compared to acetylcholine is due to slow ionic diffusion through the inhibitor, which give rise to the deposition of inhibitor molecules close to the surface of the Cu – Sn - Zn – Pb Alloy (Shahzad *et al.*, 2020; Solomon *et al.*, 2020; Tamalmani and Husin, 2020), hence greater inhibition efficiency as already

recorded in the weight loss and electrochemical approaches. To identify the most reactive sites (local reactivity) in both rivastigmine and acetylcholine, the condensed Fukui functions of rivastigmine and acetylcholine inhibitors was examined. The maximum positive magnitudes of Fukui Functions for Rivastigmine are located on C8, C10, C11, C15 and N9. Contrarily, maximum negative magnitudes of Fukui functions are on C15, C17, N14 and O18. In the acetylcholine inhibitor, the maximum positive magnitudes of Fukui functions are located on C3, C6, C7, N2, and O8 while the maximum negative magnitudes of Fukui functions are located on C1, C4, C10 and O5.

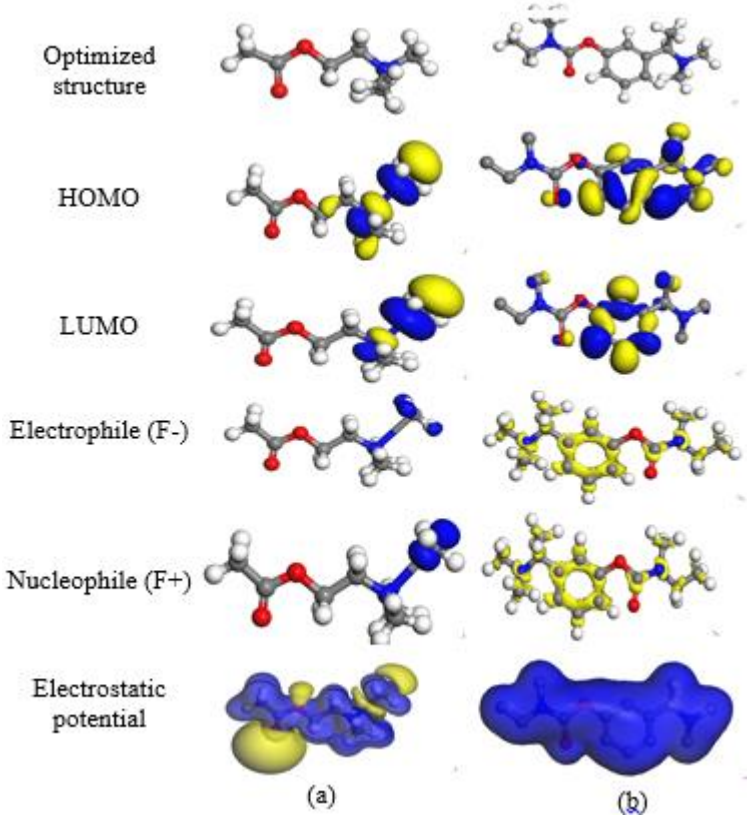

Fig. 4. Chemical structures, optimized, HOMO, LUMO, Fukui functions and ESP images of rivastigmine and acetylcholine expired drugs using DFT

Table 4 Quantum chemical calculation parameters for the inhibition of Cu – Sn - Zn – Pb Alloy surface by (a) ACC and (b) RVM in HCl environment

Parameters	Acetylcholine (ACC)	Rivastigmine (RVM)
Binding energy (ev)	-2500.5 kcal/mol (-108.4 eV)	-3635.1 kcal/mol (-157.6 eV)
E_{HOMO} (eV)	-4.208 eV	-5.691 eV
E_{LUMO} (eV)	-2.269 eV	-5.145 eV
Energy gap (ΔE) (eV)	-1.939 eV	-0.546 eV
Global hardness	-0.970 eV	-0.273 eV
Global softness	-0.516 eV	-1.831 eV

Thermodynamics approach: From Table 5, the values of activation energy were seen to be increasing with increased inhibitor concentrations. An indication that both inhibitors established a strong energy barrier at the metal/inhibitor interface such that it opposes the speedy corrosion reaction process (Obot *et al.,* 2019; McCafferty 2010; Ogunleye *et al.,* 2020). Ea values were found to be higher in the inhibited solution compared to the non-inhibited solution and less than 20 $kJmol^{-1}$. This explained a possible decrease in inhibition efficiency with increase temperature and physical adsorption process (Rodic and Milosey 2019; Ngobiri *et al.,* 2019). Values of enthalpy in Table 5 were negative which explains an exothermic reaction[14-16]. An indication that more and stronger bonds were formed between the inhibitor molecules and those of the Cu – Sn - Zn – Pb alloy, hence creating a stronger adsorption and surface coverage (Ogunleye *et al.,* 2020. It has been known that ΔH_{ads} values < 80 $kJmol^{-1}$ represent a physical adsorption mechanism by the inhibitors and this values were obtained for the inhibitors. The reaction also shows decreasing disorderliness of the reaction as values of the entropy of adsorption were decreasing with inhibitor concentration owing to the replacement of water molecules from the inhibitors.

Table 5. Thermodynamics parameters for the inhibition of Cu – Sn - Zn – Pb Alloy surface in HCl environment

	Acetylcholine (ACC)			Rivastigmine (RVM)		
Conc.	Ea	ΔHads (kJ/mol)	ΔSads (kJ/mol)	Ea	ΔHads (kJ/mol)	ΔSads (kJ/mol)
Blank	5.8	-7.9	-73.0	5.8	-7.9	**-73.0**
300 ppm	10.8	-14.5	-139.6	11.0	-14.8	-138.0
500 ppm	11.3	-15.7	-148.0	12.2	-16.7	-153.1
700 ppm	11.6	-15.5	-156.7	12.9	-16.7	-157.3
900 ppm	12.4	-17.9	-166.7	13.3	-17.3	-161.6
1500 ppm	15.0	-20.8	-206.9	14.8	-15.4	-181.1

Langmuir adsorption estimation: In determining the nature of adsorption of the inhibitor on the surface of Cu – Sn - Zn – Pb alloy, Langmuir adsorption isotherm was tested. Table 6 displayed the Langmuir adsorption parameters. It is observed that a perfect linear regression coefficient (R^2) was obtained when data was fitted into the linear Langmuir isotherm model, showing that both rivastigmine and acetylcholine adsorption was consistent with the Langmuir adsorption isotherm model, hence a monolayer physical adsorption process (Sehmi *et al.,* 2020; Tamalmani and Husin 2020; Ugi *et al.,* 2020). The relationship between C and C/Θ gave straight lines, and adsorption - desorption equilibrium constant was determined from the intercept. The standard free energy of adsorption ΔG_{ads} was obtained from Eq (10)

$$K_{ads} = \frac{1}{55.5} exp\left(\frac{-\Delta G_{ads}}{RT}\right)\ldots \qquad (10)$$

Where R is the universal gas constant, and the value 55.55 is the water concentration in the solution (mol L^{-1}).

Higher values of K_{ads} with corresponding lower values of ΔG_{ads} indicate a strong interaction and adsorption on the metal surface (Shahzad *et al.,* 2020; Ugi *et al.,* 2020; Wang *et al.,* 2019[a]; 2019[b]). Hence, rivastigmine and acetylcholine exhibited a strong interaction with the Cu – Sn - Zn – Pb Alloy surface.

Table 6. Langmuir isotherm results for the inhibition of Cu – Sn - Zn – Pb Alloy surface by rivastigmine and acetylcholine inhibitors in HCl environment

	Acetylcholine (ACC)			Rivastigmine (RVM)		
Temp. (K)	k (mol/L)	R^2	ΔG^*_{ads} (kJ/mol)	k (mol/L)	R^2	ΔG^*_{ads} (kJ/mol)
303	0.0028	0.9896	-22.091	0.0032	0.9961	-21.755
313	0.0040	0.9893	-21.892	0.0038	0.9947	-22.026
333	0.0054	0.9958	-22.461	0.0054	0.996	-22.461

SEM: The monographs displayed in Fig. 5a present a surface morphology of Cu – Sn - Zn – Pb alloy after immersion in 1.5 M HCl solution without rivastigmine and acetylcholine inhibitors for 12 h through the Scanning Electron Microscope (SEM). As seen in Fig. 5a, the SEM image revealed surface damage owing to the aggressive attack of the HCl solution (Majda *et al.,* 2020; McCafferty 2010; Ngobiri *et al.,* 2019). On the contrary, the surface of the Cu – Sn - Zn – Pb alloy immersed in the inhibited solutions for 12 h with 300 and 1500 ppm (Fig. 5b – e) shows a significant reduction in surface damage. From the micrographs, it could be said that there is adsorption of inhibitor molecules on the active sites of the Cu – Sn - Zn – Pb alloy, which resulted in a smoother surface (except for a few spots), indicating the inhibition of the metal from corrosion (Wilfred *et al.,* 2020).

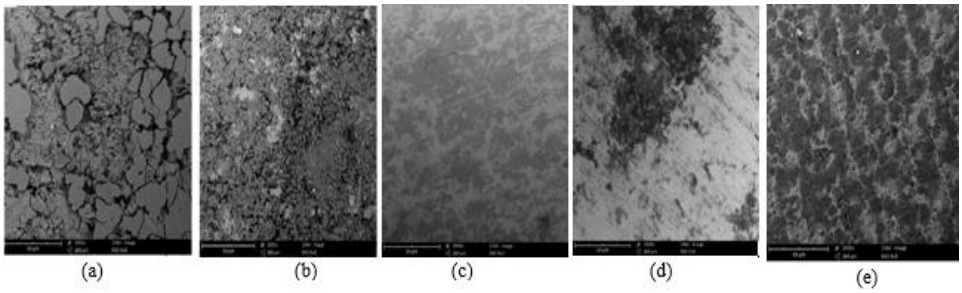

Fig. 5. Micrographs for Cu – Sn - Zn – Pb Alloy in (a) Blank HCl (b) 300 ppm RVM (c) 1500 ppm RVM (d) 300 ACC and (e) 1500 ppm ACC

Conclusion: Research findings showed that Cu – Sn - Zn – Pb Alloy surface was perfectly inhibited by both rivastigmine and acetylcholine expired drugs in HCl environment with % IE at 99.1 and 95.0 %. Inhibition was by adsorption of the inhibitor (rivastigmine and acetylcholine) molecules on the metal surface and substituting of water molecules. Inhibition reaction was exothermic allowing for stronger bond formation between the rivastigmine and acetylcholine inhibitors and Cu – Sn - Zn – Pb Alloy surface hence building a stronger inhibition efficiency. It was also found out that the inhibitors were stabled, their reaction was spontaneous in the forward direction, physically adsorbed and mixed type. Inhibitors were able to

improve on the charge transfer resistance and corrosion current densities, and reduce the double layer capacitance in the electrochemical process.

REFERENCES

Ammen, CW (2000). *Metalcasting*. McGraw-Hill Professional, p. 133.

Brady, M; George, S; Clauser, HR; John, AV (2002). *Materials Handbook*. McGraw-Hill Professional, p. 468–469.

Dagdag, O; El Harfi, A; Cherkaoui, O; Safi, Z; Wazzan, LG; Akpan, ED (2019). Rheologilocal, electrochemical, surface, DFT and molecular dynamics simulation studies on the anticorrosive properties of new epoxy monomer compound for steel in 1 M HCl solution, *RSC Advances*, 9: 4454-4462.

Davanya, DK; Frank, VP; Vijaya, DP (2020). Green approach to corrosion inhibition of mild steel in Hydrochloric acid by 1-[morphholin-4-yl(thiophen-2-yl)methyl]thiourea. *J. fail. Analys. prev.*, 20: 494 – 502.

Davis, JR (2000). *Corrosion: Understanding the basics.* ASM Int. pub. USA, p. 93 – 106.

European Copper Institute. (2018). *Gunmetal*. Intl. Copper Assoc. Pub. Belgium, p. 27

Faiza, M; Zahari, A; Awanga, K; Hussin, H (2020). Corrosion inhibition on mild steel in 1 M HCl solution by Cryptocarya nigra extracts and three of its constituents (alkaloids). *RSC Adv.*, 10: 6547-6562.

Gergely, A (2019.) *Phenomenal theories in corrosion science: Methods of prevention*. Nova Pub., USA: p. 39

Go, LC; Depan, D; Holmes, WE; Gallo, A; Knierim, K; Bertrand, T; Hernandez, R (2020). Kinetic and thermodynamic analyses of the corrosion inhibition of synthetic extracellular polymeric substances, *Peer J Mat. Sc.*, 2: (2020), e4

Idouhli, R; Koumya, Y; Khadiri, M (2019). Inhibitory effect of Senecio anteuphorbium as green corrosion inhibitor for S300 steel, *Int J Ind Chem.*, 10: 133–143

Majda, MT; Ramezanzadeh, M; Ramezanzadeh, B; Bahlakeh, G (2020). Production of an environmentally stable anti-corrosion film based on Esfand seed extract molecules- metal cations: Integrated experimental and computer modeling approaches, *J. Hazard. Mat.*, 382: 1-16.

McCafferty, E (2010). *Introduction to corrosion science.* Springer Pub, UK, p. 96

Ngobiri, NC; Oguzie, EE; Oforka, NC; Akaranta, O (2019). Comparative study on the inhibitive effect of Sulfadoxine–Pyrimethamine and an industrial inhibitor on the corrosion of pipeline steel in petroleum pipeline water. *Arabian J. Chem.*, 12: 1024-1034.

Obot, IB; Umoren, SA; Ankah, NK (2019). Pyrazine derivatives as green oil field corrosion inhibitors for steel. *J. Mol. Liq.*, 277: 749–61.

Ogunleye, OO; Arinkoola, AO; Eletta, OA; Agbede, OO; Osho, YA; Morakinyo, A F; Hamed, JO (2020). Green corrosion inhibition and adsorption characteristics of Luffa cylindrica leaf extract on mild steel in hydrochloric acid environment. *Eliyon*, 6(1): e03205.

Rodic, P; Milosev, I (2019). The influence of additional salts on corrosion inhibition by cerium (III) acetate in the protection of AA 7075-T6 in chloride solution. *Corr. Sc.*, 149: 108-122.

Sangeetha, C; Chinnakani, S (2020). Jatropha gossyfolia – A green inhibitor act as anticorrosive agent on carbon steel. *J. Adv. Sci. Res.*, 11: 1-9

Sehmi, A; Ouici, HB; Guendouzi, A; Ferhat, M; Benali, O; Boudjellal, F (2020). Corrosion Inhibition of Mild Steel by newly Synthesized Pyrazole Carboxamide Derivatives in HCl Acid Medium: Experimental and Theoretical Studies. *J. Electrochem. Soc.*, 167(15): 23 - 33

Shahzad, K; Sliem, M; Shakoor, RA (2020). Electrochemical and thermodynamic study on the corrosion performance of API X120 steel in 3.5% NaCl solution. *Sci. Rep.*, 10: 4314

Singh, P; Chauhan, DS; Chauhand, SS; Singha, G; Quraishi, MA (2019). Chemically modified expired Dapsone drug as environmentally benign corrosion inhibitor for mild steel in sulphuric acid useful for industrial pickling process, *J. Mol. Liq.*, 286(15): 110903

Solomon, MM; Umoren, SA; Quraishia, MA; Tripathi, D; Abai, EJ, (2020). Effect of akyl chain length, flow, and temperature on the corrosion inhibition 1 of carbon 2 steel in a simulated acidizing environment by an imidazoline-based inhibitor, *J. Petrol. Sc. Eng.*, 1-39

Tamalmani, K; Husin, H (2020). Review on Corrosion Inhibitors for Oil and Gas Corrosion Issues, Appl. *Sci.*,10(10): 3389

Ugi, BU; Bassey, VM; Obeten, ME; Adalikwu, SA; Nandi, DO (2020). Secondary Plant Metabolites of Natural Product Origin - Strongylodon macrobotrys as Pitting Cor-rosion Inhibitors of Steel around Heavy Salt Deposits in Gabu, Nigeria. *J. Mat. Sci. Chem. Engr.,* 8(5): 38 – 60.

Wang, C; Chen, J; Han, J; Wang, C; Hu, B (2019). Enhanced corrosion inhibition performance of novel modified polyaspartic acid on carbon steel in HCl solution. *J. Alloys Comp.,* 771: 736–746

Wang, Q; Tan, B; Bao, H; Xie, Y; Mou, Y; Li, P; Chen, D; Shi, Y; Li, X; Yang W (2019). Evaluation of Ficus tikoua leaves extract as an eco-friendly corrosion inhibitor for carbon steel in HCl media *Bioelectrochemistry*, 128: 49-55

Wilfred, E; Run-Hua, Z; Okafor, PC; Xing-Wen, Z; He, KW; Xiu-Zhou, L; Chun-Ru, C (2020). Adsorption and corrosion inhibition performance of multi-phytoconstituents from Dioscorea septemloba on carbon steel in acidic media: Characterization, experimental and theoretical studies, *Colloids and Surfaces A: Physicochem. Eng. Aspects*, 590(5): 124534